Pergamon

Scripta Materialia, Vol. 38, No. 10, pp. 1481–1485, 1998
Elsevier Science Ltd
Copyright © 1998 Acta Metallurgica Inc.
Printed in the USA. All rights reserved.
1359-6462/98 $19.00 + .00

PII S1359-6462(98)00089-X

COMPARISON OF THE CORROSION BEHAVIOR OF A BULK AMORPHOUS METAL, $Zr_{41.2}Ti_{13.8}Cu_{12.5}Ni_{10}Be_{22.5}$, WITH ITS CRYSTALLIZED FORM

V. Schroeder, C.J. Gilbert and R.O. Ritchie
Department of Materials Science and Mineral Engineering, University of California, Berkeley, CA 94720-1760

(Received February 20, 1998)
(Accepted March 4, 1998)

Introduction

Since the discovery of the first metallic glass in 1960 (1), amorphous metals have been made in a variety of compositions. However, they have been largely fabricated as thin ribbons less than a millimeter in thickness because fast cooling rates ($\sim 10^6$ K/sec) have been required to retain the metastable amorphous phase. Recently, however, a new class of amorphous metals has been developed which require cooling rates of only 1 K/sec (2); these alloys, such as $Zr_{41.2}Ti_{13.8}Cu_{12.5}Ni_{10}Be_{22.5}$ (at%), can thus be processed in bulk form.

Amorphous metals have generated much interest, both in basic research and for structural applications, because of their near-theoretical strength to stiffness ratios and extremely low damping characteristics (3). In addition, a number of amorphous metals exhibit excellent corrosion resistance (4–7), which has been explained in terms of their structural homogeneity. Since amorphous metals are in principle structurally and chemically homogeneous and thus lack any microstructure, such as grain boundaries, which could act as local electrochemically-active sites, many researchers attribute "good corrosion resistance" to the entire class of amorphous metals. It is this point, whether the amorphous condition itself confers improved corrosion resistance, that we examine in the present note.

Background

The tendency of a metal to passivate depends on alloy composition and solution chemistry. Consequently, the corrosion resistance of amorphous metals also depends on these two factors. Passivating iron-based alloys with substantial additions of chromium and molybdenum exhibit superior corrosion resistance in the amorphous state in comparison to the crystalline alloy in a variety of aqueous solutions (8–10). Moreover, iron-tungsten amorphous alloys exhibit superior corrosion resistance in acidic solutions, but not in neutral or basic solutions (11). Although the presence of a passive film is necessary for excellent corrosion resistance of an amorphous metal, it is not the only criterion. Copper/zirconium, for instance, is a passivating alloy that has nearly identical corrosion behavior in the amorphous and crystalline form (12). Also, iron passivates in many solutions, but when alloyed only with a metalloid (B, C, P), amorphous iron does not exhibit superior corrosion resistance compared to the crystalline alloy of the same composition (13). To explain such behavior, it has been suggested that for the

amorphous alloys which exhibit excellent corrosion properties, the passive films that form are very stable and repassivate quickly if the film is damaged (14,15).

Since it is the alloy composition and not the amorphous state *per se* that dictates the corrosion properties of amorphous metals, each amorphous alloy must be investigated separately to determine its corrosion behavior. In this regard, the corrosion properties of the recently developed bulk amorphous alloy, $Zr_{41.2}Ti_{13.8}Cu_{12.5}Ni_{10}Be_{22.5}$ (at%), have not been investigated. In this study, the corrosion behavior of both the amorphous and crystalline forms of the bulk alloy are investigated in aqueous sodium chloride and sodium perchlorate solutions to investigate their resistance to localized pitting corrosion and general corrosion.

Experimental Procedure

As-received $7 \times 40 \times 40$ mm^3 plates of $Zr_{41.2}Ti_{13.8}Cu_{12.5}Ni_{10}Be_{22.5}$ (at%) (Amorphous Technologies, Corp.) were machined into $3 \times 3 \times 50$ mm^3 beams. One 3×50 mm^2 surface was polished to a 1-μm finish (Acroscope, Santa Clara, CA). Due to the beryllium content, samples were not additionally polished immediately prior to experiments. The fully crystallized version of the alloy was produced by heat treating as-received specimens *in vacuo* ($\sim 10^{-6}$ Torr) at 450°C for 24 h (see the time-temperature-transformation diagram in Ref. 16). The microstructure is described elsewhere (17,18), as well as the x-ray diffraction data from the as-received and the heat treated metal (19). Electrical connection was made to the electrodes with an aluminum alloy wire, attached to the sample with silver epoxy. On the polished surface, a 2.5×4 mm^2 portion was exposed, while the rest of the sample was protected with Miccrostop (Tolber, Hope, AR).

During electrochemical experiments, the potential was controlled by an EG&G Model 363 potentiostat/galvanostat, and was ramped anodically or cathodically from the corrosion potential with an MTS 410 digital function generator. The potential and current were recorded on an HP 7090A measurement plotting system, and later digitized. As-quenched (fully amorphous) or annealed (fully crystalline) electrodes were introduced into an aerated 0.5 M NaCl solution (98+%, Aldrich) or 0.5 M $NaClO_4$ solution (99+%, EM Science) under potential control. The potential was maintained at -2500 mV (SCE) for 5 min to reduce any air-formed oxide with a saturated calomel reference electrode (SCE) and a platinum counter electrode. The sample was then left at open circuit for 20 min, at which time a value for the corrosion potential was recorded. From the corrosion potential, the electrode was scanned cathodically or anodically at 1 mV/sec.

A Perkin-Elmer Auger electron spectroscopy system was used to examine the air-formed oxide on the amorphous alloy. In order to determine the presence of specific elements in the oxide film, layers of the oxide were removed by sputtering with a focused gallium ion beam (FEI single lens power supply); the resulting high intensity peaks at defined energies were compared to the peaks for standards containing Zr, Ti, Cu, Ni, Be, O, and C.

Results and Discussion

Representative plots of the cathodic and anodic potentiodynamic polarizations of $Zr_{41.2}Ti_{13.8}Cu_{12.5}Ni_{10}Be_{22.5}$ amorphous and crystalline electrodes in 0.5 M NaCl are displayed in Fig. 1. The significant features on these plots are the corrosion and pitting potentials for the amorphous and crystalline electrodes. For the crystalline structure, the average corrosion potential is -316 mV (SCE) with a variation of ~ 60 mV in eight experiments, and the average pitting potential is -227 mV with a variation of ~ 40 mV in four experiments. Both the corrosion potential and the pitting potential are located at higher potentials for the amorphous structure; specifically, the average corrosion potential is

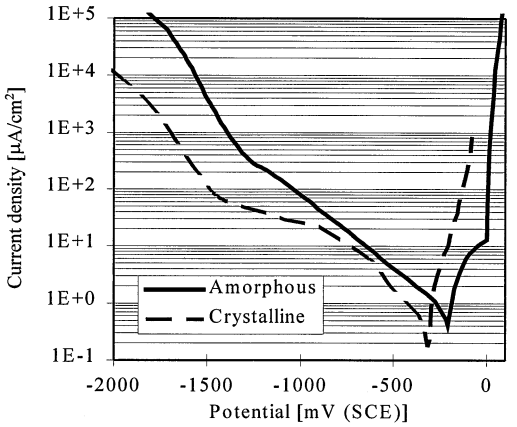

Figure 1. Anodic and cathodic potentiodynamic polarizations of amorphous (—) and crystalline (– –) $Zr_{41.2}Ti_{13.8}Cu_{12.5}Ni_{10}Be_{22.5}$ (at%) structures in 0.5 M NaCl solution.

−205 mV (eight experiments) and the average pitting potential is +2 mV (four experiments) with a variation of ~30 mV and ~35 mV, respectively.

After anodic potentiodynamic polarizations in sodium chloride solution, the surfaces of the crystalline and amorphous electrodes exhibited sporadically distributed, non-uniformally sized corrosion pits, which had low aspect ratios without any undercutting of the side walls. The corrosion pits on the amorphous metal were non-uniformally shaped, while the pits on the crystalline metal were approximately round polygons with variable numbers of sides.

In 0.5 M $NaClO_4$ solution, representative potentiodynamic polarization curves exhibit similar values of corrosion potential for crystalline and amorphous electrodes (Fig. 2). The corrosion potentials, averaged over six experiments, are −265 mV for the amorphous electrode and −290 mV for the crystalline electrode. In six experiments, the values for corrosion potential varied by ~50 mV and ~60 mV, respectively. In addition, the anodic current recorded during experiments varied by less than an order of magnitude for the two types of structures.

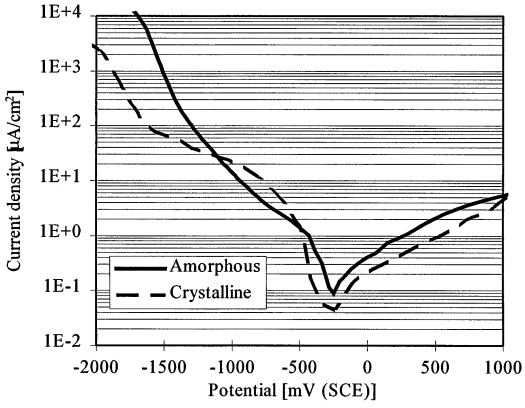

Figure 2. Anodic and cathodic potentiodynamic polarizations of amorphous (—) and crystalline (– –) $Zr_{41.2}Ti_{13.8}Cu_{12.5}Ni_{10}Be_{22.5}$ (at%) structures in 0.5 M $NaClO_4$ solution.

In both aqueous solutions, the anodic and cathodic potentiodynamic polarizations do not reflect the growth or reduction of oxidized species on the surface of the alloys. However, considering the Pourbaix diagrams for the pure constituent metals (20), and the behavior of titanium (21) and zirconium (22) in other alloys, an oxide film is most likely formed on the alloy surface. In addition, preliminary Auger electron spectroscopy results suggest that all components of the Zr-Ti-Cu-Ni-Be alloy are present in the air-formed oxide.

While an oxide film is most likely present during anodic polarizations, the amorphous phase (with a pitting potential of $\Delta\Phi_{pit} \sim +2$ mV) is only slightly more resistant to pitting corrosion than the crystalline alloy ($\Delta\Phi_{pit} \sim -227$ mV); in addition, it does not exhibit the superior corrosion resistance observed in other amorphous alloys (4–7). The pitting potential of the amorphous alloy may also be compared to that of zirconium and titanium, which have the largest elemental weight fractions in the alloy. For example, pure titanium has superior pitting resistance in air-saturated, 1N NaCl, in which corrosion pits nucleate between 11.2 V and 11.6 V (SCE) (23). On the other hand, pure zirconium in aerated 0.5 M NaCl has a pit nucleation potential (obtained galvanostatically) of ~160 mV (SCE) (24, 25), which is only slightly more resistant to pitting than the amorphous metal. Comparing the pitting potential of the amorphous metal to the crystalline metal of the same composition, to pure zirconium, and to pure titanium, it is clear that the amorphous metal does not have superior resistance to pitting corrosion in sodium chloride. In addition, the similar values of anodic current in the sodium perchlorate solution suggest that the amorphous alloy is no more resistant to general corrosion in sodium perchlorate than the crystalline material. From the values of pitting potential and anodic current, it can be inferred that the oxide films formed in sodium perchlorate and sodium chloride solutions do not give amorphous $Zr_{41.2}Ti_{13.8}Cu_{12.5}Ni_{10}Be_{22.5}$ superior corrosion properties; the corrosion properties of the amorphous metal more likely result from slow repassivation at sites of film damage (14,15).

Conclusions

Based on the results of the potentiodynamic polarizations of crystalline and amorphous electrodes of the bulk amorphous metal alloy, $Zr_{41.2}Ti_{13.8}Cu_{12.5}Ni_{10}Be_{22.5}$, in 0.5 M NaCl and 0.5 M $NaClO_4$ solutions, it can be concluded that the amorphous structure is only slightly more resistant to pitting corrosion than the corresponding crystalline structure in NaCl, and is no more resistant to general corrosion in $NaClO_4$. Thus, the homogeneity of the surface of the amorphous phase *per se* does not significantly improve the resistance of the $Zr_{41.2}Ti_{13.8}Cu_{12.5}Ni_{10}Be_{22.5}$ (at%) alloy to general or localized corrosion.

Acknowledgments

This work was supported by the U.S. Air Force Office of Scientific Research under Grant No. F49620-1-0365 with additional support from Amorphous Technologies, Corp., and Howmet, Corp. Thanks are due to Drs. A. Peker and M. Tenhover (Amorphous Technologies) for providing the alloy and to Prof. W. L. Johnson for helpful discussions.

References

1. W. Klement, R. H. Willens, and P. Duwez, Nature 187, 869 (1960).
2. A. Peker and W. L. Johnson, Appl. Phys. Lett. 63, 2342 (1993).
3. J. J. Gilman, J. Appl. Phys. 46, 1625 (1975).
4. M. Naka, K. Hashimoto, and T. Masumoto, Corrosion. 32, 146 (1976).
5. T. M. Devine, J. Electrochem. Soc. 124, 1 (1977).

6. A. N. Mansour and C. A. Melendres, J. Electrochem. Soc. 142, 1961 (1995).
7. T. Ramchandran and T. K. G. Namboodhiri, Corrosion. 40, 73 (1984).
8. M.-W. Tan, E. Akiyama, A. Kawashima, K. Asami, and K. Hashimoto, Corros. Sci. 38, 349 (1996).
9. K. Asami, M. Naka, K. Hashimoto, and T. Masumoto, J. Electrochem. Soc. 127, 2130 (1980).
10. R. B. Diegle, Corrosion. 35, 250 (1979).
11. S. Yao, S. Zhao, L. Ren, H. Guo, and M. Kowaka, Surf. Coat. Technol. 79, 205 (1996).
12. J. C. Turn, Jr. and R. M. Latanision, Corrosion. 39, 271 (1983).
13. M. Naka, K. Hashimoto, and T. Masumoto, J. Non-crystall. Sol. 31, 355 (1979).
14. K. Hashimoto, in Passivity of Metals and Semiconductors, ed. M. Froment, p. 235, Elsevier Science Publishers, Amsterdam, The Netherlands (1984).
15. S. Virtanen and H. Bohni, Corros. Sci. 31, 333 (1990).
16. A. Peker and W. L. Johnson, Mater. Sci. Eng. A179/A180, 173 (1994).
17. S. Schneider, P. Thiyagarajan, and W. L. Johnson, Appl. Phys. Lett. 68, 493 (1996).
18. R. Busch, S. Schneider, and W. L. Johnson, Appl. Phys. Lett. 67, 1544 (1995).
19. C. J. Gilbert, R. O. Ritchie, and W. L. Johnson, Appl. Phys. Lett. 71, 476 (1997).
20. M. Pourbaix, in Atlas of Electrochemical Equilibria in Aqueous Solution, Pergamon Press, Oxford, UK (1966).
21. D. G. Kolman and J. R. Scully, J. Electrochem. Soc. 143, 1847 (1996).
22. M. Janik-Czachor, Corrosion. 49, 763 (1993).
23. H.-J. Raetzer-Scheibe, Corrosion. 12, 437 (1978).
24. N. Hackerman and O. B. Cecil, J. Electrochem. Soc. 101, 419 (1954).
25. D. R. Knittel and A. Bronson, Corrosion. 40, 9 (1984).